



Precursory patterns to vortex nucleation in stirred Bose-Einstein condensates

Jonas Rønning  and Luiza Angheluta 

The Njord Center, Department of Physics, University of Oslo, Blindern, 0316 Oslo, Norway



(Received 26 October 2022; accepted 25 April 2023; published 18 May 2023)

Within the Gross-Pitaevskii theory, we study precursory pattern formations to the nucleation of vortex dipoles in a two-dimensional Bose-Einstein condensate stirred by a Gaussian potential. We introduce a smooth superfluid vorticity field and its conservative current, which capture very well the gradual process of vortex nucleation as a mechanism of topological singularities acquiring smooth cores. This is characterized by the localization of the superfluid vorticity into core regions which harbor the phase slips. For more impenetrable obstacles, we find that there are additional phase slips that do not acquire cores, thus remaining pinned as ghost vortices to the potential. We show that the vortex kinematics is slaved to the superfluid vorticity current, which determines not only the onset of nucleation but also the shedding dynamics.

DOI: [10.1103/PhysRevResearch.5.023108](https://doi.org/10.1103/PhysRevResearch.5.023108)

I. INTRODUCTION

Topological defects are the fingerprints of broken continuous symmetries and are widely encountered in ordered systems, such as disclinations in liquid crystals [1,2], dislocations in solid crystals [3–5], orientational defects in biological active matter [6–8], quantized vortices in quantum fluids [9–11], or cosmic strings [12]. The formation and dynamics of topological defects during phase ordering kinetics through temperature quenches from the disordered phase have been well studied for decades [13]. Going beyond the relaxation to equilibrium, more recent theoretical approaches have focused on the collective behavior in driven ordered systems through the dynamics of topological defects.

The topological defects in an atomic Bose-Einstein condensate (BEC) are quantum vortices where the condensate is locally melted while losing its phase coherence. This induces persistent circulating superfluid flow about the vortex cores [14]. With the advent of tailored experimental realizations of BECs comes also a surge in theoretical studies focused on understanding and tracking nonthermal nucleation and dynamics of quantized vortices in driven Bose-Einstein condensates. Two main frameworks are currently applied to study the vortex nucleation in two-dimensional BECs, either by rotating the condensate [15–17] or by coupling the condensate with a moving obstacle [18–22]. The nucleation criterion is based on the energetic argument that the superfluid flow reaches a critical velocity above which the condensate phase gradient undergoes phase slips. In rotating BEC systems, vortices of the same circulation are created when the total amount of angular momentum exceeds a critical threshold for the vortex formation. Same-sign vortices form at the edge of the

condensate and migrate into the bulk, where they eventually form vortex lattices after reequilibration [15,23–26].

The vortex nucleation in condensates stirred by a moving obstacle has also been studied [27–31] and observed experimentally [21,22]. Here, the nucleation criterion relies on the height U_0 of the repulsive Gaussian potential representing the coupling of the stirring obstacle to the condensate. A hard potential corresponds to an almost impenetrable obstacle when $U_0 > \mu$, where μ is the chemical potential, such that the condensate density rapidly decreases and nearly vanishes inside the potential. By contrast, a soft potential corresponds to a penetrable obstacle for $U_0 < \mu$ such that the condensate density is gently depleted inside the obstacle. The onset of vortex nucleation induced by a hard obstacle occurs when the local condensate velocity reaches the critical velocity for phonon emission, whereas for the soft obstacle this is a necessary but not a sufficient requirement [27,28]. Stirring obstacles are typically modelled as Gaussian potentials with varying height and width [30,31]. In Ref. [31] the vortex nucleation induced by a repulsive Gaussian potential of different strengths is studied numerically. It is found that near the critical velocity for vortex nucleation, the energy gap between the ground state and the excited state goes to zero as a power law, while ghost vortices, i.e., phase slips, are formed inside the potential. By contrast, no such ghost vortices develop in the case of soft potentials. In addition to tuning the degree of permeability of the obstacle, different vortex shedding regimes, from vortex dipoles, pairs, and clusters [32–34], can be induced by varying the size of the obstacle through the width of the potential, which also changes the critical stirring velocity [21,35]. Once vortices are being shed into the condensate they interact with each other, forming dynamic clusters that sustain energy cascades and two-dimensional quantum turbulence [11,34,36–39].

Even though compressibility effects, due to shock waves and phonons, are particularly important in the nucleation and the annihilation of vortex dipoles, they are typically overlooked in the quantum turbulence regime where turbulent

Published by the American Physical Society under the terms of the Creative Commons Attribution 4.0 International license. Further distribution of this work must maintain attribution to the author(s) and the published article's title, journal citation, and DOI.

energy spectra and clustering behavior is attributed mostly to the mutual interactions between vortices [37,40]. The point vortex modeling approach has been employed to characterize different quantum turbulence regimes [41–45]. In point vortex models, vortices are reduced to charged point particles with an overdamped dynamics where their velocity is determined by the mutual interaction potential or external potentials. While the point vortex approach is suitable for studying collective vortex dynamics, it cannot model fast processes such as vortex annihilation or creation events without ad hoc rules since, by construction, it overlooks the finite vortex core and compressibility effects, which are crucial to fast events.

An accurate, nonperturbative method of deriving the velocity of topological defects directly from the evolution of the order parameter of the O(2) broken rotational symmetry has been developed by Halperin and Mazenko [46–48]. Topological defects are located as zeros in the 2D vector order parameter, where the magnitude of order vanishes to regularize the core region where the phase of the order parameter becomes undefined. The defect velocity is determined by the magnitude of the defect density current at the defect position. In the frozen-phase approximation, where the phase of the order parameter is stationary apart from its moving singularities, the vortex kinematics determined by the evolution of the order parameter reduces to a point vortex model [45,47]. Within the Gross-Pitaevskii theory, the order parameter is the condensate wave function, and the frozen-phase approximation is the regime where the dynamics of phonon modes can be neglected. This is a versatile formalism which has been applied to various systems, from tracking of point dislocations [4] and dislocation lines [5] in crystals, point orientational defects in active nematics [49] and active polar systems [50], disclination lines in nematic liquid crystals [51] and vortex lines in BECs [52].

In this paper we adopt the Halperin-Mazenko formalism to gain further theoretical insights into the process of vortex nucleation as a mechanism by which phase singularities acquire a finite core to form a vortex. In Sec. II we present this formalism for two-dimensional (2D) BECs and show that the defect density field D represents a generalized, smooth vorticity, defined as the curl of the superfluid current, and its evolution determines the vortex velocity. This method circumvents the need of operating directly with the singularities in the condensate phase, which are harder to manipulate both theoretically and numerically. In Sec. III we study the pattern formations developed in the superfluid vorticity D and its current density $\mathbf{J}^{(D)}$ during the nucleation process and show that the superfluid vorticity condensed into well-defined cores which harbor phase slips. In Sec. IV we show that the superfluid vorticity current which determines vortex dynamics reduces to the point vortex model in the frozen-phase approximation and derive the kinematics of point vortices in the presence of both superfluid flow and nonuniform condensate density. Concluding remarks and a summary are presented in Sec. V.

II. VORTICES AS MOVING ZEROS

The superfluid flow and the topological structure of a weakly interacting BEC are described by the evolution of

its macroscopic wave function $\psi = |\psi|e^{i\theta}$, where $|\psi|$ is the magnitude of the condensate wave function and θ is the condensate phase. Disturbances in the condensate phase generate a superfluid flow with a current (momentum) density

$$\mathcal{J} = |\psi|^2 \nabla \theta = \text{Im}(\psi^* \nabla \psi), \quad (1)$$

such that gradients in the condensate phase define the superfluid flow velocity, which is irrotational everywhere except at the points \mathbf{r}_α where the condensate phase loses its coherence and becomes undetermined (singular), namely,

$$\nabla \times \nabla \theta = 2\pi q_\alpha \delta^2(\mathbf{r} - \mathbf{r}_\alpha). \quad (2)$$

This phase singularity has a topological nature determined by a $2\pi q_\alpha$ phase jump upon going counterclockwise around a loop C_α enclosing it, where $q_\alpha = \pm 1$ is the topological charge of the lowest energy quantum vortex, namely,

$$2\pi q_\alpha = \oint_{C_\alpha} d\theta = \oint_{C_\alpha} d\mathbf{l} \cdot \nabla \theta, \quad (3)$$

which is equivalent to the differential form in Eq. (2). Thus, for configurations of well-separated vortices punctuating an otherwise uniform condensate, the singular vortex charge density field is a superposition of δ functions centered at the vortex positions,

$$\rho_v(\mathbf{r}, t) = \sum_\alpha q_\alpha \delta^2[\mathbf{r} - \mathbf{r}^{(\alpha)}(t)], \quad (4)$$

and it represents the singular vorticity field as the curl of the superfluid flow velocity. From the single-valuedness of the condensate wave function everywhere, it follows that the condensate density vanishes where the condensate phase is undetermined. Hence, quantum vortices are located at zeros of the condensate wave function ψ as exploited by Halperin and Mazenko [46,47]. By representing the complex ψ field as an O(2)-symmetric real vector field $\vec{\Psi} = [\Psi_1; \Psi_2]$, where $\Psi_1 = \text{Re}(\psi)$ and $\Psi_2 = \text{Im}(\psi)$, we notice that $\vec{\Psi}(\mathbf{r})$ maps a point \mathbf{r} to a point in the (Ψ_1, Ψ_2) disk centered at the origin and of unit radius (i.e., the uniform condensate density in rescaled units). Regions of uniform condensate density map to the unit circle, whereas vortices located at various positions \mathbf{r}_α in the real space reside at the origin of the (Ψ_1, Ψ_2) disk. The coordinate transformation between the physical (x, y) space to the (Ψ_1, Ψ_2) disk is determined by the Jacobi determinant

$$D = \begin{vmatrix} \partial_x \Psi_1 & \partial_x \Psi_2 \\ \partial_y \Psi_1 & \partial_y \Psi_2 \end{vmatrix} = \epsilon_{ij} \partial_i \Psi_1 \partial_j \Psi_2 = \frac{\epsilon_{ij}}{2i} \partial_i \psi^* \partial_j \psi, \quad (5)$$

where ϵ_{ij} is the Levi-Civita tensor and Einstein's summation convention is used. The D field is a scalar field that vanishes in regions of uniform condensate phase and is non zero otherwise, as it is the case around vortices. By a coordinate transformation of the Dirac δ function in Eq. (4), we can rewrite the singular vortex density in terms of the zeros of the $\vec{\Psi}$ as

$$\rho_v(\mathbf{r}, t) = D(\mathbf{r}, t) \delta^2(\vec{\Psi}). \quad (6)$$

In fact, the D field is a measure of the nonsingular vorticity as the curl of the superfluid current [52]

$$\epsilon_{ij} \partial_j \mathcal{J}_i = \epsilon_{ij} \text{Im}(\partial_i \psi^* \partial_j \psi) = 2D. \quad (7)$$

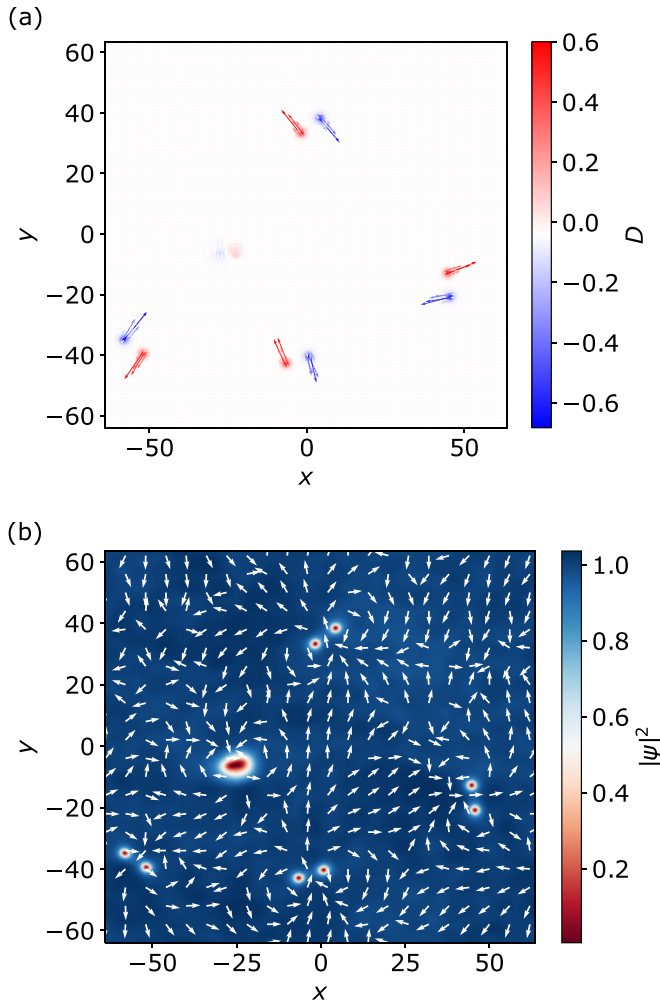


FIG. 1. Snapshot of (a) D field and (b) condensate density $|\psi|^2$ around a stirring Gaussian potential when vortex dipoles are being shed. The vector fields are (a) defect current $\mathbf{J}^{(D)}$ and (b) director of the superfluid current \mathcal{J} , respectively. Negative vortices move in the opposite direction of $\mathbf{J}^{(D)}$. System size is represented in units of the healing length.

This is also reflected in the fact that the singular, topological structure in the condensate phase is regularized by vanishing density which introduces a finite core size of the condensate vortices. The D field as a superfluid vorticity locates both the core and the circulation of the vortices as illustrated in Fig. 1(a). To show that the D field indeed captures the topological phase slips, we integrate Eq. (7) over an area S containing vortices

$$\int_S d^2\mathbf{r}D = \frac{1}{2} \int_{\partial S} d\mathbf{l} \cdot \mathcal{J} = \frac{1}{2} \int_{\partial S} |\psi|^2 \nabla\theta \cdot d\mathbf{l}. \quad (8)$$

In the assumption that the contour ∂S enclosing the area S is sufficiently far away from well-separated vortices, i.e., the superfluid density equals its uniform bulk value $|\psi_0|^2 = 1$ along the integration contour, the above integral reduces to

$$\int_S d^2\mathbf{r}D = \pi \sum_{\alpha \in S} q_\alpha, \quad (9)$$

where the sum is over all vortices inside the contour. Equivalently, integrating the absolute value of D , we obtain instead the total number N of vortices enclosed by the contour,

$$\int_S d^2\mathbf{r}|D| = \sum_{\alpha} q_{\alpha} \int_{S_{\alpha}} d^2\mathbf{r}D = N\pi, \quad (10)$$

which is the limit case of a uniform condensate punctuated by well-separated vortices.

However, the generalized vorticity D field picks up not only topological defects but any phase gradient (flow) disturbances modulated by the superfluid density, which may be induced by compressible modes, trapping, or stirring potentials. These nonsingular contributions become particularly important for the nucleation of vortices as discussed in Sec. III and have been overlooked in earlier studies using the Halperin-Mazenko formalism.

Flow disturbances with a topological origin can be dissociated from the rest by the value of the generalized vorticity determined by the condensate density profile near a vortex. Namely, if we consider Eq. (8) for a disk S of radius much smaller than the healing length and centered at an isolated vortex in an otherwise homogeneous condensate, we find that the value of the D field reaches in magnitude a value given by

$$|D_0| = \Lambda^2 \approx 0.7, \quad (11)$$

using the near-vortex profile of the condensate $|\psi|(r) = \Lambda r$ [53], and the numerical value for the steepness Λ of the density gradients taken from Ref. [39].

This superfluid vorticity is a topologically conserved quantity given by [47]

$$\partial_t D = -\partial_i J_i^{(D)}, \quad (12)$$

with its corresponding superfluid vorticity current

$$J_i^{(D)} = \epsilon_{ij} \text{Im}(\partial_i \psi \partial_j \psi^*), \quad (13)$$

determined uniquely by the evolution of the ψ field and accurately tracking the motion of the vortices as also illustrated in Fig. 1(a) for a snapshot of a stirred condensate with several dipoles. This current density is nonzero where the superfluid flow is nonuniform, particularly through the vortex cores where there are phase slips, as seen in Fig. 1(a). Figure 1(b) represents a color map of condensate density and the vector field of the normalized superfluid current showing vortical flow around vortices for the same snapshot as in panel (a). The Gaussian stirring potential is the larger indentation in the condensate density.

When the D field tracks vortices, it determines the topological invariance of the singular defect charge density ρ_v , namely, that

$$\partial_t \rho_v = -\partial_i J_i^{(\rho_v)}, \quad (14)$$

with the corresponding singular vortex current density being (see Appendix)

$$\begin{aligned} \mathbf{J}^{(\rho_v)}(\mathbf{r}, t) &= \mathbf{J}^{(D)}(\mathbf{r}, t) \delta^2(\vec{\Psi}) \\ &= \sum_{\alpha} q_{\alpha} \frac{\mathbf{J}^{(D)}(\mathbf{r}_{\alpha})}{D(\mathbf{r}_{\alpha})} \delta^2(\mathbf{r} - \mathbf{r}_{\alpha}). \end{aligned} \quad (15)$$

In the frozen-phase approximation, the vortex core is rigid and the equilibrium vortex wave-function profile remains stationary in the vortex comoving frame. In this case the vortex current is identical to the advective current $\sum_{\alpha} q_{\alpha} \mathbf{v}_{\alpha} \delta^2(\mathbf{r} - \mathbf{r}_{\alpha})$ [54]. Within this approximation, the velocity is uniform or slowly varying through the vortex core and given as

$$\mathbf{v}_{\alpha} = \frac{\mathbf{J}^{(D)}(\mathbf{r}_{\alpha})}{D(\mathbf{r}_{\alpha})}. \quad (16)$$

This relation provides an accurate measurement of the vortex velocity and can be reduced to the point vortex model as discussed further in Sec. IV. Within the Gross-Pitaevskii theory, the evolution of the condensate wave function ψ in the presence of a potential field $U(\mathbf{r}, t)$ containing both a static trapping potential and a time-dependent stirring potential can be described by a damped Gross-Pitaevskii equation (dGPE), which in dimensionless units reads as [11,38,39]

$$\partial_t \psi = (i + \gamma) \left[\frac{1}{2} \nabla^2 \psi + (1 - U - |\psi|^2) \psi \right], \quad (17)$$

where the damping coefficient γ is an effective thermal drag that represents the coupling of the condensate with a static thermal bath and particle exchanges [55]. The dimensional units used in the rescaling are given by the chemical potential μ , the healing length $\xi = \hbar/\sqrt{m\mu}$ and the sound velocity $c = \mu/m$. The wave function is rescaled in units of $\sqrt{\mu/g}$, where m is the mass of the bosons and g is an effective scattering parameter for the interactions between bosons.

By inserting Eq. (17) into the conservation law of the D field in Eq. (12), we express the evolution of the generalized superfluid vorticity as

$$\begin{aligned} \partial_t D = & -\frac{1}{2} \epsilon_{ij} \partial_i \partial_k \text{Re}(\partial_k \psi^* \partial_j \psi) + \frac{\epsilon_{ij}}{2} \partial_i U \partial_j |\psi|^2 \\ & + \frac{\gamma}{2} \nabla^2 D + 2\gamma D [1 - U - 2|\psi|^2] \\ & + \gamma \mathcal{J} \cdot \nabla^{\perp} U + \frac{\gamma}{2} \epsilon_{ij} \text{Im}[\partial_i \partial_k \psi \partial_j \partial_k \psi^*]. \end{aligned} \quad (18)$$

The first term on rhs is a sink/source superfluid vorticity coming from the kinetic energy. The second term corresponds to the coupling with an external potential and gives a nonzero contribution (as a sink/source) only when the gradient in the condensate density is normal to the gradient force. The remaining terms are the different contributions of the thermal damping to the dissipation of superfluid vorticity, such as diffusion, sink/sources from the coupling with a potential U , and a thermal drag induced by superfluid flow.

Since the condensate density vanishes at the vortex position, the only nonzero contribution to the generalized vorticity current density at the vortex position comes from the kinetic energy; thus the general formula for the vortex velocity can be expressed as

$$\mathbf{v}_{\alpha} = i \frac{\text{Re}(\nabla^2 \psi^* \nabla^{\perp} \psi) + \gamma \text{Im}(\nabla^2 \psi \nabla^{\perp} \psi^*)}{\nabla \psi^* \cdot \nabla^{\perp} \psi} \Bigg|_{\mathbf{r}=\mathbf{r}_{\alpha}}, \quad (19)$$

and reduces in certain approximations to the point vortex dynamics as detailed in Sec. IV. However, the sink/source contribution from the external potential U plays an important role in the nucleation and shedding of vortices as discussed next.

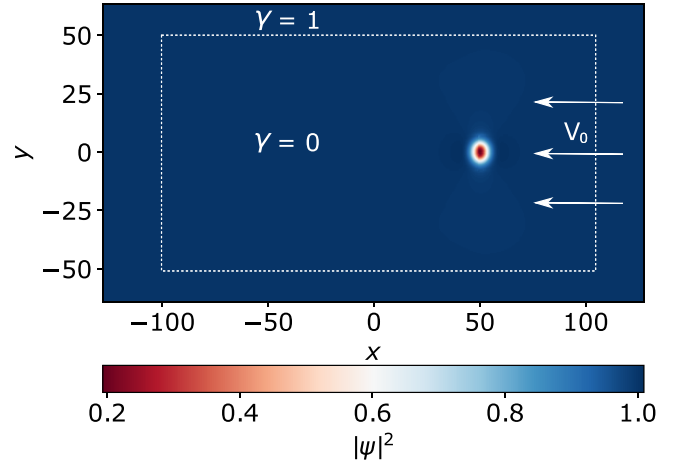


FIG. 2. Numerical setup of the condensate in the comoving frame of the Gaussian potential (uniform flow direction shown by the arrows). The color map represents the condensate density. The dotted lines show the thermal buffer interfaces.

III. VORTEX NUCLEATION

To study the onset of vortex nucleation, we consider a uniform Bose-Einstein condensate at zero temperature that is coupled with a Gaussian potential moving at a constant speed V_0 along the x axis. Using the Galilean invariance of the GPE at $\gamma = 0$, we can transform it to the comoving frame by boosting the wave function with the phase factor $\exp(iV_0 x + i\frac{V_0^2}{2} t)$ to account for the shift in the kinetic energy [56]. The form of the GPE is invariant under Galilean transformation only when $\gamma = 0$.

In the comoving frame, this is equivalent to having a static potential in a uniform superfluid flow described by

$$\partial_t \psi + V_0 \partial_x \psi = i \left[\frac{1}{2} \nabla^2 + (1 - |\psi|^2) - U_0 e^{-\frac{(x-x_0)^2}{d^2}} \right] \psi, \quad (20)$$

where d is the width of the potential and U_0 is the coupling strength.

In numerical simulations we consider a thermal buffer on the edge of the periodic domain where the damping coefficient is nonzero to avoid recirculation of the shed vortex dipoles and to dampen wave interference as illustrated in Fig. 2. A similar computational trick was used in previous studies of the vortex shedding [33] and the formation of a phonon wake [56]. The width of the stirring potential is set to $d = 4$, and we vary its speed V_0 and its height U_0 . We use a rectangular domain $[-128, 128] \times [-64, 64]$ (corresponding to a 512×256 rectangular grid) and a fixed time step $dt = 0.01$. The potential is centered in the middle of the domain at $(x_0, y_0) = (50, 0)$. For the dissipative buffer we set the thermal drag to $\gamma(\mathbf{r}) = \max[\gamma_x(x), \gamma_y(y)]$, which is effectively equal to 1, as shown in Fig. 2. The smooth, but sharp transition between the buffer and bulk values is mediated by the interfacial profiles along the x and y directions given by

$$\gamma_x(x) = \frac{1}{2} (2 + \tanh[(x - w_x)/\Delta] - \tanh[(x + w_x)/\Delta]),$$

and similarly for $\gamma_y(y)$. Here $x = \pm w_x$ and $y = \pm w_y$ locate the positions of the top and bottom buffer interfaces along

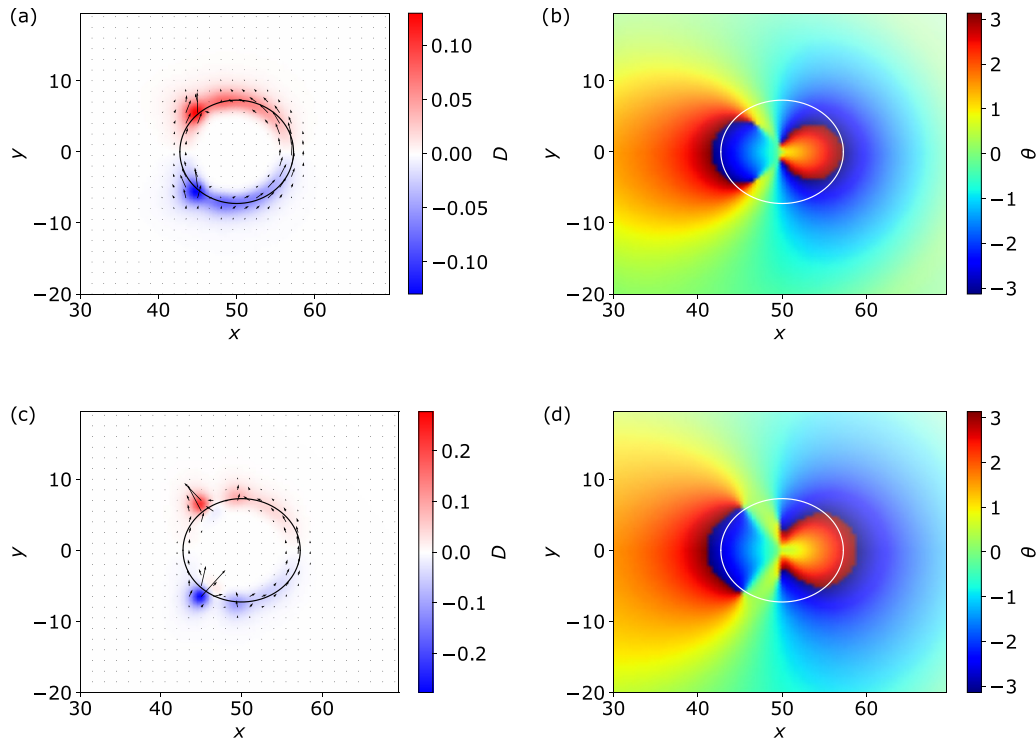


FIG. 3. (a) D field and (b) condensate phase θ around a hard potential at $t = 19$ prior to a nucleation. Two dipoles of phase slips reside inside the potential. (c) D field and (d) θ at $t = 28$ (at the nucleation onset) when one dipole of phase slips have migrated to occupy the two vorticity blobs. White/black circle is the radius where the potential becomes e^{-1} . The vector field in (a), and (c) represents the superfluid vorticity current. The potential strength is $U_0 = 10$, and the stirring speed is $V_0 = 0.4$, slightly above the estimated critical speed for this value of U_0 , $V_{0c} \approx 0.38$.

the x direction, while Δ is the width of interface. The buffer parameters are set to $w_x = 100$, $w_y = 50$, and $\Delta = 7$.

We start by relaxing the initial Thomas-Fermi ground state in imaginary time to find the steady state at $V_0 = 0$ and then evolve the condensate wave function according to Eq. (20) for a given V_0 . However, since the initial state is not the ground state of this equation, there will be an initial disturbance forming around the potential which may lead to defect nucleation even below the critical velocity. Thus we first let the system relax this initial disturbance before we analyze the nucleation process. The regime with $U_0 > 1$ (in units of the chemical potential) corresponds to a hard potential whereby the condensate density almost vanishes inside the obstacle, akin to the homogeneous boundary condition imposed at an impenetrable boundary which melts the condensate phase coherence at any stirring velocity. Conversely, for soft-indenting potentials equivalent to $U_0 < 1$, the condensate density is more gently depleted such that phase coherence is preserved below a critical speed. The transition from soft to hard potential obstacle occurs around $U_0 \sim 1$, where the potential induces a dipole of phase slips pinned inside the obstacle [35].

The superfluid vorticity D field and its current density turn out to be advantageous tools to unravel and explore the distinct precursory patterns to the onset of vortex nucleation and shedding for different stirring conditions as discussed next. For hard potentials, one dipole of phase slips develops and remained pinned inside the obstacle where the condensate density is close to zero for stirring velocities above and slightly below the critical value as visualized in Figs. 3(b)

and 3(d) (above the critical velocity) and Fig. 4(b) (below the critical velocity). However, it turns out that the presence of this dipole does not necessarily lead to nucleation. From the profile of the superfluid vorticity D field around the stirring potential, we can get a more in-depth understanding of the dynamical pattern formation leading to the nucleation of a vortex dipole. Below the critical speed we observe that a steady-state profile of the superfluid vorticity concentrated in a diffuse halo surrounding the edge of the potential such that the circulation changes sign symmetrically about the direction of motion as shown the Fig. 4(a). In this steady state, the superfluid vorticity current vanishes and results in no shedding event, even though there is one dipole of phase slips pinned in the middle of the potential [see Fig. 4(b)]. For this reason, this dipole was also termed as a ghost vortice in Ref. [31]. Above the critical velocity, which depends on U_0 as studied in Ref. [35], there is no steady state in the superfluid vorticity. Instead, the diffusive halo around the potential tends to localize over time into two blobs of opposite circulation as shown in Figs. 3(a) and 3(c), corresponding to the formation of two vortex cores. While the cores are forming on the edge, two dipoles of phase slips have formed inside the potential, where one detaches and migrates towards the vorticity cores while the other stays pinned. The onset of vortex nucleation corresponds to the moment when the two vorticity cores are hosting one phase slip each. The subsequent vortex shedding is precisely determined by the D -field current, which endows the vortices with a net velocity away from the potential as shown in Fig. 3(c). Thus the vortex shedding pattern and frequency could be further studied from

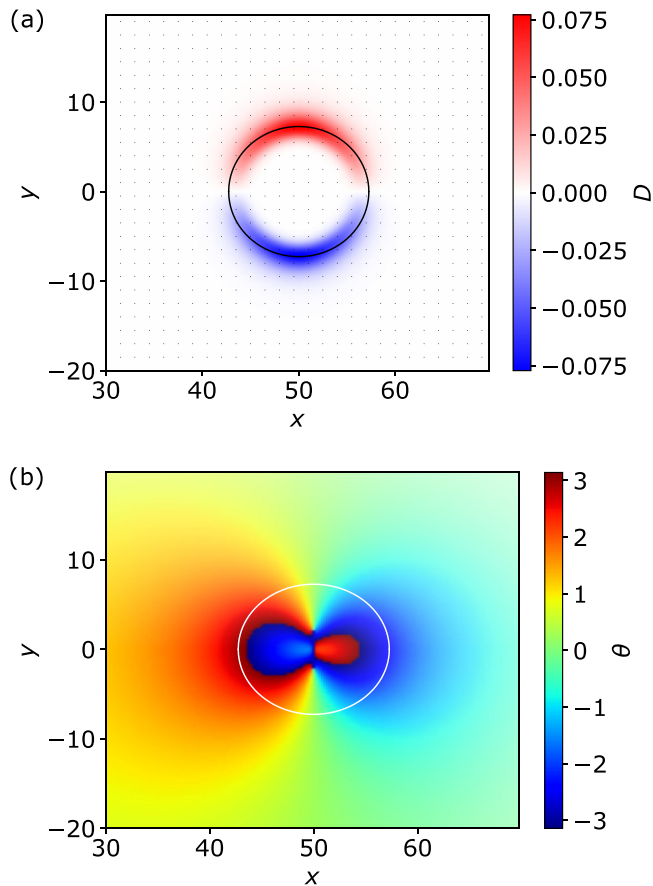


FIG. 4. (a) Steady-state profile of the D field for a hard potential $U_0 = 10$ with the stirring speed $V_0 = 0.35$ (below the critical value). (b) Ghost dipole of phase slips inside the hard obstacle.

the D -field current. We also note that this formalism allows us to make a clear distinction between real versus ghost vortices. The latter are really due to the hard potential breaking the phase coherence. It is the second dipole of phase slips which controls the nucleation process.

As argued earlier, the important distinction of soft and hard potentials is the presence of ghost vortices. The D field is a powerful tool to further investigate the influence of ghost vortices on the nucleation mechanism, which is a challenging task. We can do this by contrasting it with the scenario where there are no ghost vortices, as is the case for soft-indenting potentials. Here, the D field develops two smeared-out regions of superfluid vorticity with alternating circulating and spanning the stirring potential. This is accompanied by smooth phase gradients as shown in Figs. 5(a) and 5(b). The locations of the regions with opposite superfluid vorticity are determined by the phase gradients through the curl of the superfluid current, as predicted by Eq. (7). Below a critical speed, this D -field pattern remains stable with its corresponding vorticity current $\mathbf{J}^{(D)}$ vanishing as illustrated in Fig. 6. Notice that the pattern in the D field is also symmetric about the direction of motion, which also determines the orientation of the phase-slip dipole. At sufficiently high V_0 a dipole of phase slips forms inside the soft potential and corresponds to the localization of the D field around two blobs with opposite circulation [Figs. 5(c) and 5(d)]. Interestingly, in this case the phase slips develop already

inside the vorticity cores to form vortices. Since the D -field current tracks the motion of these vortices, it also reveals the direction in which vortices are being shed, as shown in Fig. 5(c).

Based on this analysis, we get new insights into the vortex nucleation as a fundamental gradual process of topological singularities acquiring a finite core. This basic mechanism is common to both hard and soft potentials. The main difference is that for the soft potential, the phase slips develop inside the vorticity core, whereas for the hard potential, the phase slips form inside the potential and migrate to vorticity cores. In this case phase slips can form as ghost vortices without there being any vorticity localization, as seen in Fig. 4(b). We have considered the homogeneous vortex nucleation and shedding away from a stirring potential in a uniform condensate. Because of the symmetry of the initial configuration, only dipoles are being nucleated and shed. However, a small noise added to the uniform condensate wave function breaks the symmetry of the initial state and may lead to vortex nucleation beyond simple dipoles [32,33]. The nucleation event remains symmetrical through the formation of dipoles of phase slips inside the potential. However, the shedding can become more irregular depending on the noise amplitude and stirring velocity.

To get a more quantitative measure of the nucleation event, we use the spatial average of the magnitude of the generalized vorticity $|D|$ as a proxy to the total number of nucleated vortices. The deviation from the theoretical prediction from Eq. (10) corresponding to a uniform superfluid punctuated by well-separated vortices informs us about the presence of additional density heterogeneities due to compressible modes or induced by the obstacle potential, as discussed earlier and shown in Figs. 3–5. In Fig. 7 we have plotted this global measure as a function of time for a soft versus hard potential and for different stirring speeds. The integration domain is a square surrounding the obstacle of size $l = 40$, i.e., the same domain that is shown in Figs. 3–6.

Below the critical speed $V_0 < V_{0c}$, the net circulation plateaus at a value lower than the predicted threshold for vortices. This corresponds to the regime where superfluid vorticity is smeared diffusively around the potential in the absence of any phase slips or vortex nucleation, as is the case for soft potentials and illustrated in Fig. 7(a).

As V_0 approaches the critical speed from below (in the absence of noise), the net circulation reaches above the 2π threshold, signaling the presence of a vortex dipole. This is common to both soft and hard potentials as shown in Figs. 7(a) and 7(b). Once the nucleated vortex dipole drifts out of the integration domain, the value of the circulation drops and shows only the contribution of the vorticity around the potential. When $V_0 > V_{0c}$, the gradual process of phase slips acquiring finite cores becomes recurrent and results in repeating vortex nucleation and shedding. Periodic shedding is observed near the critical speed, and more irregular shedding occurs with higher speeds, as shown in Figs. 7(a) and 7(b).

IV. VORTEX KINEMATICS

Using the formalism presented in Sec. II, we now derive a closed expression for the vortex kinematics in the presence

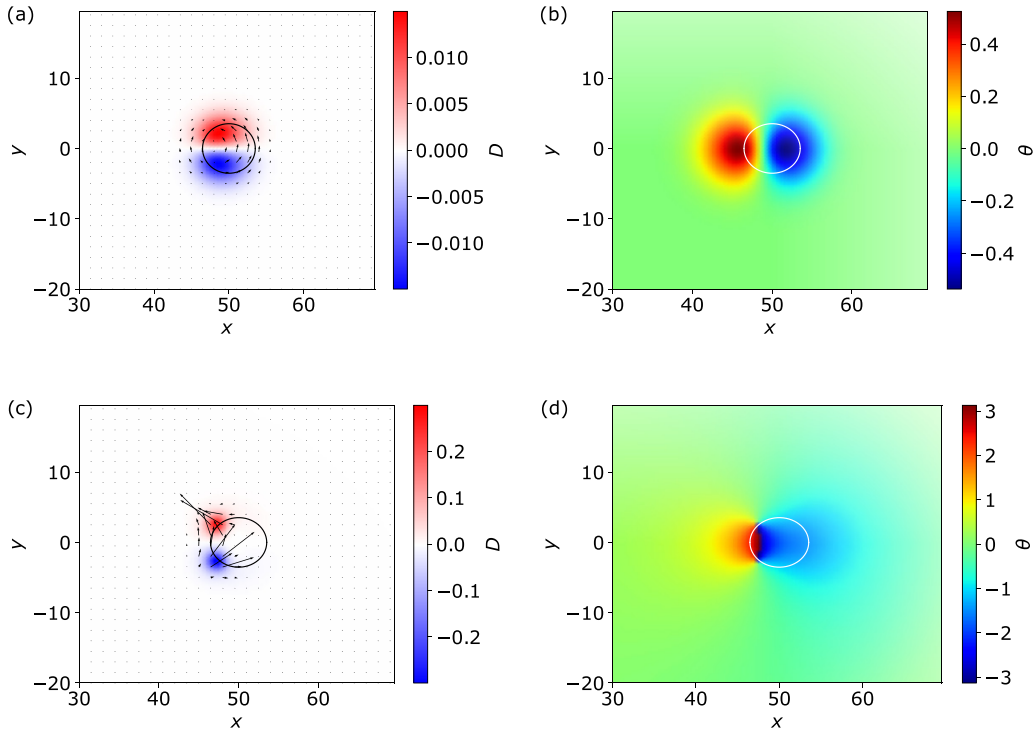


FIG. 5. D field with defect current (a), (c) and condensate phase (b), (d) around the soft potential during a dipole nucleation. Before the phase slips formed, $t = 5$ (a), (b), the D field spreads diffusively inside the potential. This region condenses into two cores which detach from the potential after they acquire phase slips at $t = 29$ (c), (d). Potential strength is $U_0 = 0.8$ and stirring speed is $V_0 = 0.42$, slightly above the estimated critical value $V_{0c} \approx 0.4$.

of both background superfluid flow and heterogeneities in the condensate density. In this section we also consider the dissipative effect of the thermal drag on the vortex dynamics. First we consider a uniform condensate punctuated at the origin with a vortex. The profile of the condensate wave function near the defect is approximated as $\psi_0 \approx r e^{iq\theta}$, where r is the distance to the vortex with circulation $q = \pm 1$ and $r \ll 1$, which is a solution of the stationary vortex, $\partial_t \psi_0 = 0$. We now introduce a smooth phase perturbation $\psi(\mathbf{r}, t) = \psi_0(\mathbf{r}) e^{i\phi(\mathbf{r}, t)}$ which accounts for the net superfluid flow at the vortex position while keeping the steady-state density profile. Near the defect position, the time evolution of the wave function is dominated by the kinetic energy contribution,

$$\partial_t \psi|_{\mathbf{r}=0} \approx (i + \gamma)^{\frac{1}{2}} \nabla^2 \psi = (-1 + i\gamma) \nabla \psi_0 \cdot \nabla \phi e^{i\phi}. \quad (21)$$

Thus, evaluating the vorticity current using the near-vortex evolution of the condensate wave function we arrive at the following expression:

$$J_i^{(D)} = \epsilon_{ij} [-\epsilon_{jk} D + \gamma q \epsilon_{kl} \epsilon_{jk} D] \partial_k \phi, \quad (22)$$

which together with Eq. (16) implies that the vortex velocity is determined by the phase gradients,

$$v_i = (\partial_i \phi + \gamma q \epsilon_{ij} \partial_j \phi)_{\mathbf{r}=0}, \quad (23)$$

which is the basic overdamped vortex dynamics in the point vortex model [57,58]. However, this model does not include the effect of condensate density disturbances due to the presence of trapping or stirring potentials.

We now apply the same method to compute the contribution of density variations to the vortex velocity. For this, the wave function is perturbed both in magnitude and phase:

$\psi = \psi_0 e^{\lambda + i\phi}$, where ϕ and λ are smooth real fields [45,48]. The generalized vorticity D field acquires an additional contribution from the density perturbations and is given by

$$D = e^{2\lambda} \frac{1}{2i} \epsilon_{ij} \partial_i \psi_0 \partial_j \psi_0. \quad (24)$$

The corresponding vortex velocity becomes

$$v_i = (\partial_i \phi - \gamma \partial_i \lambda + \gamma q \epsilon_{ij} \partial_j \phi + q \epsilon_{ij} \partial_j \lambda)_{\mathbf{r}=0}, \quad (25)$$

which is consistent with the dissipative vortex dynamics obtained by a different approach in Ref. [59]. A similar dissipative dynamics in the absence of density variations has also been used in Ref. [60] to study the diffusive expansion of a vortex cluster and compare with experimental observations. This equation reduces to the expressions obtained in Refs. [45,48] for $\gamma = 0$. In Ref. [45] it was shown that the density inhomogeneities due to an harmonic trap induces an orbital motion or a vortex imprinted in the condensate. This is precisely determined by last term in Eq. (25) due to the spatial profile of the condensate density. The effect of thermal drag is that it makes oppositely charged vortices attract each other according to the third term in Eq. (25). Also, vortices move down gradients in the background condensate density as given by the second term. For the harmonic trap this implies that vortices have instead a spiral motion towards the edge of the trap.

To illustrate this we track the trajectory of a single vortex imprinted in a BEC coupled to a harmonic potential. At zero temperature the vortex moves in a orbit of constant radius around the center of the harmonic trap. As a dissipative effect of the effective thermal drag, the vortex acquires a radial

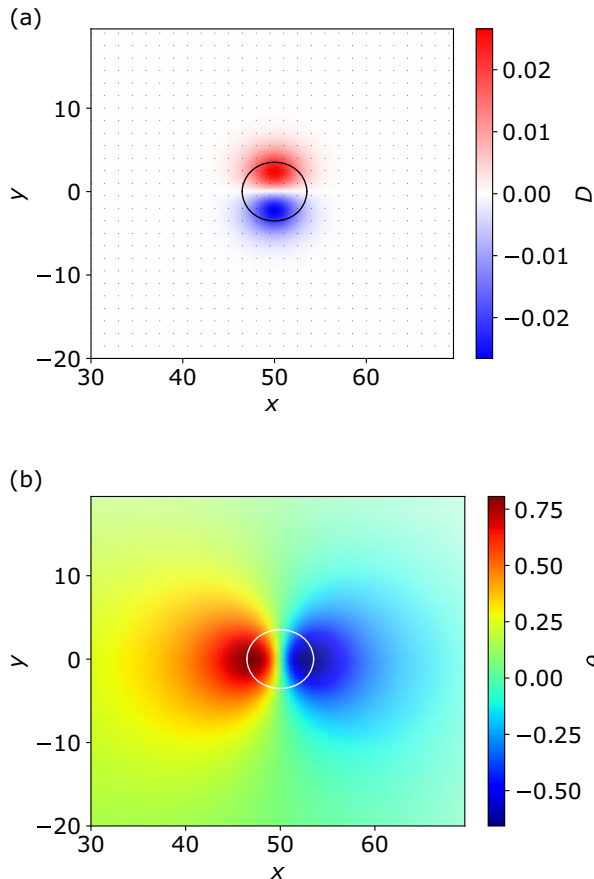


FIG. 6. (a) Steady-state profile of the D field for a soft potential $U_0 = 0.8$ at velocity $V_0 = 0.38$ (below the estimated critical value ≈ 0.4). (b) Smooth-steady-state profile of the condensate phase.

velocity and spirals out towards the edge of the trap. The angular v_θ and radial v_r velocity components as functions of time are shown in Fig. 8. We notice that velocity obtained by the slope of the vortex trajectory is a noisy signal compared to the velocity from Eq. (16).

V. DISCUSSION AND CONCLUSIONS

In summary, we have extended the Halperin-Mazenko formalism to characterize the nucleation and dynamics of vortices in a stirred Bose-Einstein condensate. We introduce a smooth superfluid vorticity D field as a topologically conserved quantity with its associated current density which tracks all the localized disturbances in the condensate both singular (vortices) and nonsingular (shock waves and disturbances induced by external potentials).

When the uniform condensate is stirred by a Gaussian potential, the onset to vortex nucleation is signalled by the precursory pattern formations in the superfluid vorticity D field which captures the process of phase slips acquiring finite cores. The D field is nonzero only around the stirring potential, where it develops two diffusive regions with alternating vorticity distributed symmetrically about the direction of motion. This also determines the orientation of the phase slip nucleating first inside the potential. The onset to nucleation is signaled by the localization of the superfluid vorticity into two

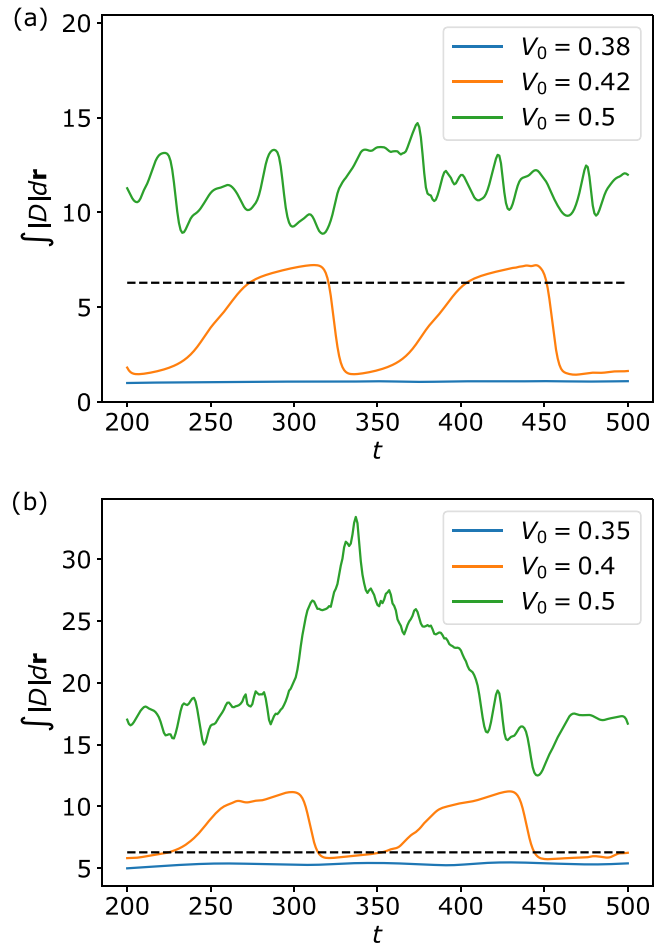


FIG. 7. Net generalized vorticity for soft potential $U_0 = 0.8$ (a) and hard potential $U_0 = 10$ (b) for different V_0 just below (blue), just above (orange), and well above (green) the critical speed. The integral is performed over the area around the potential shown in Figs. 3 and 5. The dotted line is the expected value corresponding to a single vortex dipole at the critical speed.

blobs that harbor the dipole of phase slips. While this process of acquiring a finite core occurs inside the potential, the actual nucleation is manifested into the condensate by the shedding of the vortex dipole.

In addition, for the hard potential, the D field localizes around the rim, signaling the presence of a ghost dipole of phase slips forming near and above the critical velocity. This ghost dipole is pinned to obstacle and aligns perpendicular to the stirring direction. Above the critical velocity an additional dipole of phase slips develops at the onset of nucleation and the previous ghost dipole is quickly migrating where vorticity localizes into vortex cores.

The superfluid vorticity current $\mathbf{J}^{(D)}$ plays an important role during the process of acquiring a core since it develops the vortex cores harboring phase slips. It also controls the vortex kinematics and thus is the quantity that dictates the shedding direction and frequency. From the general relation to this current density, we derive closed expressions for the vortex velocity depending on phase gradients and density disturbances. It is worth noting that the Halperin-Mazenko formalism may be extended also to analyzing experimental

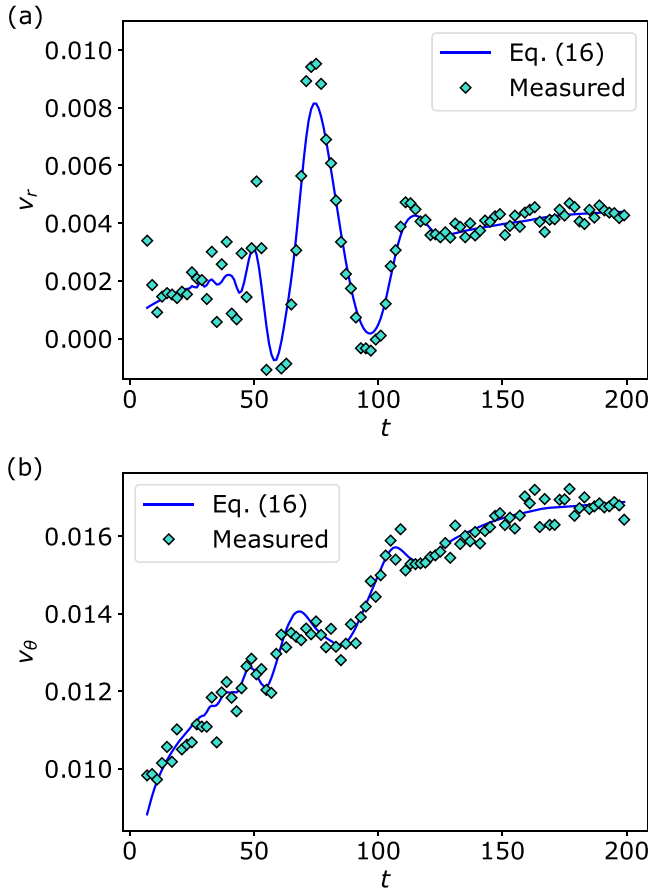


FIG. 8. (a) Radial velocity component v_r and (b) angular velocity component v_θ of a single vortex in a harmonic potential with $R_{rf} = 60$ obtained from Eq. (16) (blue line) and from tracking the position of the defect (turquoise diamonds). The thermal drag is set to $\gamma = 0.05$.

data and identifying different types of condensate disturbances.

ACKNOWLEDGMENTS

We are grateful to Vidar Skogvoll, Marco Salvalaglio, and Jorge Viñals for many fruitful discussions.

APPENDIX

Here we derive the expression of the defect density current,

$$\mathbf{J}^{(\rho_v)}(\mathbf{r}, t) = \mathbf{J}^{(D)}(\mathbf{r}, t)\delta^2(\vec{\Psi}),$$

where $\delta^2(\vec{\Psi}) = \delta(\Psi_1)\delta(\Psi_2)$. We first start by multiplying Eq. (12) with $\delta^2(\vec{\Psi})$,

$$\delta^2(\vec{\Psi})\partial_t D = -(\partial_i J_i^{(D)})\delta^2(\vec{\Psi})$$

$$\partial_t \rho_v - D\partial_t \delta^2(\vec{\Psi}) = -\partial_i (J_i^{(D)}\delta^2(\vec{\Psi})) + J_i^{(D)}\partial_i \delta^2(\vec{\Psi}), \quad (A1)$$

where the last term on the right-hand side can be expressed as

$$\begin{aligned} J_i^{(D)}\partial_i \delta^2(\vec{\Psi}) &= \epsilon_{ij}\epsilon_{kl}\partial_j \Psi_k \partial_l \Psi_l \partial_i \Psi_m \frac{d}{d\Psi_m} \delta^2(\vec{\Psi}) \\ &= \epsilon_{kl}(\epsilon_{ij}\partial_i \Psi_m \partial_j \Psi_k)\partial_l \Psi_l \frac{d}{d\Psi_m} \delta^2(\vec{\Psi}). \end{aligned} \quad (A2)$$

Note that ∂_j and ∂_i acting on the same $\vec{\Psi}$ component lead to a vanishing term due to the Levi-Civita tensor. Thus the only nonzero contributions contain $D = \epsilon_{ij}\partial_j \Psi_1 \partial_i \Psi_2$ and therefore

$$J_i^{(D)}\partial_i \delta^2(\vec{\Psi}) = -D\partial_t \delta^2(\vec{\Psi}). \quad (A3)$$

Inserting this into Eq. (A1), we arrive at

$$\partial_t \rho_v = -\partial_i (J_i^{(D)}\delta^2(\vec{\Psi})),$$

from which the current density of ρ_v follows.

[1] P. G. d. Gennes, *The Physics of Liquid Crystals*, 2nd ed., The International Series of Monographs on Physics Vol. 83 (Clarendon Press, Oxford, 1993).
 [2] P. Poulin, H. Stark, T. Lubensky, and D. Weitz, Novel colloidal interactions in anisotropic fluids, *Science* **275**, 1770 (1997).
 [3] F. C. Frank, The influence of dislocations on crystal growth, *Discuss. Faraday Soc.* **5**, 48 (1949).
 [4] A. Skaugen, L. Angheluta, and J. Viñals, Dislocation dynamics and crystal plasticity in the phase-field crystal model, *Phys. Rev. B* **97**, 054113 (2018).
 [5] V. Skogvoll, L. Angheluta, A. Skaugen, M. Salvalaglio, and J. Viñals, A phase field crystal theory of the kinematics of dislocation lines, *J. Mech. Phys. Solids* **166**, 104932 (2022).
 [6] S. P. Thampi, R. Golestanian, and J. M. Yeomans, Vorticity, defects and correlations in active turbulence, *Philos. Trans. R. Soc. A* **372**, 20130366 (2014).
 [7] A. Doostmohammadi, T. N. Shendruk, K. Thijssen, and J. M. Yeomans, Onset of meso-scale turbulence in active nematics, *Nat. Commun.* **8**, 15326 (2017).
 [8] A. Amiri, R. Mueller, and A. Doostmohammadi, Unifying polar and nematic active matter: Emergence and co-existence of

half-integer and full-integer topological defects, *J. Phys. A: Math. Theor.* **55**, 094002 (2022).
 [9] W. F. Vinen, The detection of single quanta of circulation in liquid helium II, *Proc. R. Soc. London A* **260**, 218 (1961).
 [10] I. M. Khalatnikov, *Theory of Superfluidity (Frontiers in Physics)* (W. A. Benjamin, New York, 1965).
 [11] A. Skaugen and L. Angheluta, Vortex clustering and universal scaling laws in two-dimensional quantum turbulence, *Phys. Rev. E* **93**, 032106 (2016).
 [12] R. Durrer, M. Kunz, and A. Melchiorri, Cosmic structure formation with topological defects, *Phys. Rep.* **364**, 1 (2002).
 [13] A. J. Bray, Theory of phase-ordering kinetics, *Adv. Phys.* **51**, 481 (2002).
 [14] P. G. Kevrekidis, D. J. Frantzeskakis, and R. Carretero-González, *Emergent Nonlinear Phenomena in Bose-Einstein Condensates: Theory and Experiment* (Springer Science & Business Media, 2007), Vol. 45.
 [15] J. R. Abo-Shaeer, C. Raman, J. M. Vogels, and W. Ketterle, Observation of vortex lattices in Bose-Einstein condensates, *Science* **292**, 476 (2001).

- [16] A. L. Fetter and A. A. Svidzinsky, Vortices in a trapped dilute Bose-Einstein condensate, *J. Phys.: Condens. Matter* **13**, R135 (2001).
- [17] A. L. Fetter, Rotating trapped Bose-Einstein condensates, *Rev. Mod. Phys.* **81**, 647 (2009).
- [18] C. Raman, M. Köhl, R. Onofrio, D. S. Durfee, C. E. Kuklewicz, Z. Hadzibabic, and W. Ketterle, Evidence for a Critical Velocity in a Bose-Einstein Condensed Gas, *Phys. Rev. Lett.* **83**, 2502 (1999).
- [19] R. Onofrio, C. Raman, J. M. Vogels, J. R. Abo-Shaer, A. P. Chikkatur, and W. Ketterle, Observation of Superfluid Flow in a Bose-Einstein Condensed Gas, *Phys. Rev. Lett.* **85**, 2228 (2000).
- [20] W. Weimer, K. Morgener, V. P. Singh, J. Siegl, K. Hueck, N. Luick, L. Mathey, and H. Moritz, Critical Velocity in the BEC-BCS Crossover, *Phys. Rev. Lett.* **114**, 095301 (2015).
- [21] W. J. Kwon, G. Moon, S. W. Seo, and Y.-i. Shin, Critical velocity for vortex shedding in a Bose-Einstein condensate, *Phys. Rev. A* **91**, 053615 (2015).
- [22] T. W. Neely, E. C. Samson, A. S. Bradley, M. J. Davis, and B. P. Anderson, Observation of Vortex Dipoles in an Oblate Bose-Einstein Condensate, *Phys. Rev. Lett.* **104**, 160401 (2010).
- [23] I. Coddington, P. Engels, V. Schweikhard, and E. A. Cornell, Observation of Tkachenko Oscillations in Rapidly Rotating Bose-Einstein Condensates, *Phys. Rev. Lett.* **91**, 100402 (2003).
- [24] D. Butts and D. Rokhsar, Predicted signatures of rotating Bose-Einstein condensates, *Nature (London)* **397**, 327 (1999).
- [25] G. M. Kavoulakis, B. Mottelson, and C. J. Pethick, Weakly interacting Bose-Einstein condensates under rotation, *Phys. Rev. A* **62**, 063605 (2000).
- [26] A. A. Penckwitt, R. J. Ballagh, and C. W. Gardiner, Nucleation, Growth, and Stabilization of Bose-Einstein Condensate Vortex Lattices, *Phys. Rev. Lett.* **89**, 260402 (2002).
- [27] C. Jossierand, Y. Pomeau, and S. Rica, Cavitation versus Vortex Nucleation in a Superfluid Model, *Phys. Rev. Lett.* **75**, 3150 (1995).
- [28] A. C. Newell and Y. Pomeau, Phase diffusion and phase propagation: Interesting connections, *Physica D* **87**, 216 (1995).
- [29] M. Crescimanno, C. G. Koay, R. Peterson, and R. Walsworth, Analytical estimate of the critical velocity for vortex pair creation in trapped Bose condensates, *Phys. Rev. A* **62**, 063612 (2000).
- [30] T. Aioi, T. Kadokura, T. Kishimoto, and H. Saito, Controlled Generation and Manipulation of Vortex Dipoles in a Bose-Einstein Condensate, *Phys. Rev. X* **1**, 021003 (2011).
- [31] M. Kunimi and Y. Kato, Metastability, excitations, fluctuations, and multiple-swallowtail structures of a superfluid in a Bose-Einstein condensate in the presence of a uniformly moving defect, *Phys. Rev. A* **91**, 053608 (2015).
- [32] K. Sasaki, N. Suzuki, and H. Saito, Bénard–von Kármán Vortex Street in a Bose-Einstein Condensate, *Phys. Rev. Lett.* **104**, 150404 (2010).
- [33] M. T. Reeves, T. P. Billam, B. P. Anderson, and A. S. Bradley, Identifying a Superfluid Reynolds Number via Dynamical Similarity, *Phys. Rev. Lett.* **114**, 155302 (2015).
- [34] W. J. Kwon, J. H. Kim, S. W. Seo, and Y.-i. Shin, Observation of von Kármán Vortex Street in an Atomic Superfluid Gas, *Phys. Rev. Lett.* **117**, 245301 (2016).
- [35] H. Kwak, J. H. Jung, and Y.-i. Shin, Minimum critical velocity of a Gaussian obstacle in a Bose-Einstein condensate, *Phys. Rev. A* **107**, 023310 (2022).
- [36] T. W. Neely, A. S. Bradley, E. C. Samson, S. J. Rooney, E. M. Wright, K. J. H. Law, R. Carretero-González, P. Kevrekidis, M. Davis, and B. P. Anderson, Characteristics of Two-Dimensional Quantum Turbulence in a Compressible Superfluid, *Phys. Rev. Lett.* **111**, 235301 (2013).
- [37] T. P. Billam, M. T. Reeves, B. P. Anderson, and A. S. Bradley, Onsager-Kraichnan Condensation in Decaying Two-Dimensional Quantum Turbulence, *Phys. Rev. Lett.* **112**, 145301 (2014).
- [38] M. T. Reeves, T. P. Billam, B. P. Anderson, and A. S. Bradley, Inverse Energy Cascade in Forced Two-Dimensional Quantum Turbulence, *Phys. Rev. Lett.* **110**, 104501 (2013).
- [39] A. S. Bradley and B. P. Anderson, Energy Spectra of Vortex Distributions in Two-Dimensional Quantum Turbulence, *Phys. Rev. X* **2**, 041001 (2012).
- [40] X. Yu and A. S. Bradley, Emergent Non-Eulerian Hydrodynamics of Quantum Vortices in Two Dimensions, *Phys. Rev. Lett.* **119**, 185301 (2017).
- [41] G. Hess, Angular momentum of superfluid helium in a rotating cylinder, *Phys. Rev.* **161**, 189 (1967).
- [42] S. Middelkamp, P. Torres, P. Kevrekidis, D. Frantzeskakis, R. Carretero-González, P. Schmelcher, D. Freilich, and D. Hall, Guiding-center dynamics of vortex dipoles in Bose-Einstein condensates, *Phys. Rev. A* **84**, 011605(R) (2011).
- [43] R. Navarro, R. Carretero-González, P. J. Torres, P. G. Kevrekidis, D. J. Frantzeskakis, M. W. Ray, E. Altuntaş, and D. S. Hall, Dynamics of a Few Corotating Vortices in Bose-Einstein Condensates, *Phys. Rev. Lett.* **110**, 225301 (2013).
- [44] A. Skaugen and L. Angheluta, Velocity statistics for nonuniform configurations of point vortices, *Phys. Rev. E* **93**, 042137 (2016).
- [45] A. J. Groszek, D. M. Paganin, K. Helmerson, and T. P. Simula, Motion of vortices in inhomogeneous Bose-Einstein condensates, *Phys. Rev. A* **97**, 023617 (2018).
- [46] B. Halperin, published in *Physics of Defects, Proceedings of Les Houches*, Session XXXV, 1980 NATO ASI, edited by Balian, Kléman, and Poirier (North Holland, Amsterdam, 1981).
- [47] G. F. Mazenko, Vortex Velocities in the O(n) Symmetric Time-Dependent Ginzburg-Landau Model, *Phys. Rev. Lett.* **78**, 401 (1997).
- [48] G. F. Mazenko, Defect statistics in the two-dimensional complex Ginzburg-Landau model, *Phys. Rev. E* **64**, 016110 (2001).
- [49] L. Angheluta, Z. Chen, M. C. Marchetti, and M. J. Bowick, The role of fluid flow in the dynamics of active nematic defects, *New J. Phys.* **23**, 033009 (2021).
- [50] B. H. Andersen, J. Renaud, J. Rønning, L. Angheluta, and A. Doostmohammadi, Symmetry-breaking transition between defect-free and defect-laden turbulence in polar active matter, [arXiv:2209.10916](https://arxiv.org/abs/2209.10916).
- [51] C. D. Schimming and J. Viñals, Singularity identification for the characterization of topology, geometry, and motion of nematic disclination lines, *Soft Matter* **18**, 2234 (2022).
- [52] A. Vilhois, D. Proment, and G. Krstulovic, Universal and nonuniversal aspects of vortex reconnections in superfluids, *Phys. Rev. Fluids* **2**, 044701 (2017).

- [53] L. Pismen, *Vortices in Nonlinear Fields: From Liquid Crystals to Superfluids, From Non-Equilibrium Patterns to Cosmic Strings* (Oxford University Press, Oxford, 1999).
- [54] V. Skogvoll, J. Rønning, M. Salvalaglio, and L. Angheluta, A unified field theory of topological defects and non-linear local excitations, [arXiv:2302.03035](https://arxiv.org/abs/2302.03035).
- [55] C. Gardiner and M. Davis, The stochastic Gross–Pitaevskii equation: II, *J. Phys. B: At., Mol. Opt. Phys.* **36**, 4731 (2003).
- [56] J. Rønning, A. Skaugen, E. Hernández-García, C. López, and L. Angheluta, Classical analogies for the force acting on an impurity in a Bose-Einstein condensate, *New J. Phys.* **22**, 073018 (2020).
- [57] J. H. Kim, W. J. Kwon, and Y.-i. Shin, Role of thermal friction in relaxation of turbulent Bose-Einstein condensates, *Phys. Rev. A* **94**, 033612 (2016).
- [58] A. Skaugen and L. Angheluta, Origin of the inverse energy cascade in two-dimensional quantum turbulence, *Phys. Rev. E* **95**, 052144 (2017).
- [59] O. Törnkvist and E. Schröder, Vortex Dynamics in Dissipative Systems, *Phys. Rev. Lett.* **78**, 1908 (1997).
- [60] O. R. Stockdale, M. T. Reeves, X. Yu, G. Gauthier, K. Goddard-Lee, W. P. Bowen, T. W. Neely, and M. J. Davis, Universal dynamics in the expansion of vortex clusters in a dissipative two-dimensional superfluid, *Phys. Rev. Res.* **2**, 033138 (2020).